Electronic Supplementary Material (ESI) for Journal of Materials Chemistry B.
This journal is © The Royal Society of Chemistry 2023

Supplemental files

Chopped fibers and nano-hydroxyapatite enhanced silk fibroin porous hybrid scaffolds for bone augmentation

Shue Jin [a], Xiaoxue Fu [a], Weinan Zeng [a], Anjing Chen [a], Zhenyu Luo [a], Yubao Li [b], Zongke Zhou [a,] and Jidong Li [b,*]*

[a]*Orthopedic Research Institute, Department of Orthopedics, West China Hospital, Sichuan University, Chengdu 610041, PR China*

[b]*Research Center for Nano-Biomaterials, Analytical and Testing Center, Sichuan University, Chengdu 610065, PR China*

**Corresponding author: Jidong Li, E-mall: nic1979@scu.edu.cn Tel: +86-028-85418178; Zongke Zhou, E-mail: zhouzongke@scu.edu.cn Tel: +86-028-85422570;*

Materials and methods

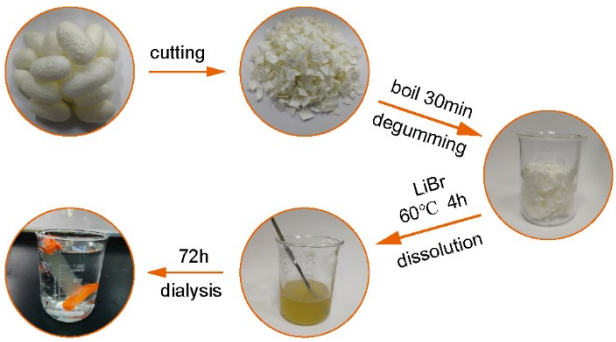

Fig. S1. The flow diagram of preparation for SF solution.

The size of n-HA was further detected by Zeta-sizer (Malvern Instruments Ltd., UK).

The enzyme-induced degradation experimental was performed to assess the stability of silk-based scaffolds. The initial mass of scaffolds was recorded as M_0. The medium was PBS buffer solution containing Protease XIV (1U/mL). Degradation conditions were set at 37 ℃ and the oscillation rate was 120 rpm/min. At a preset time-point (1, 3, and 5 day), the remaining scaffolds were collected after centrifugation, dried to constant weight, weighed and recorded at last (M). The mass loss of scaffold was calculated as $(M_0\text{-}M)/M_0 \times 100\%$.

Result and discussion

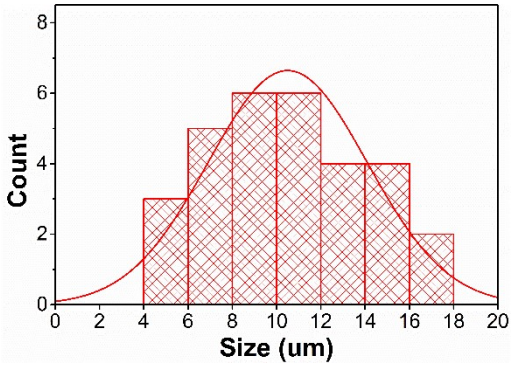

Fig. S2. The size distribution of CF.

The size distribution of n-HA was detected by Zeta-sizer. As shown in **Fig. S3**, the size of n-HA particles was 263.1 ± 12.2 nm.

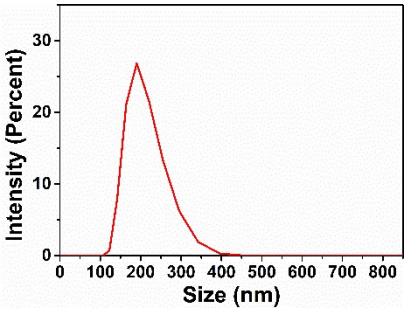

Fig. S3. The size distribution of n-HA.

The concentration of SF solution was optimized by pore structure and mechanical properties to further construct a porous hybrid scaffold. The morphology of SF porous scaffolds prepared with different concentrations (5%, 15%, and 25%) of SF solution is shown in **Fig. S4a**. The pore size of the 5%S scaffold is large, the pores are not uniform, and the pore wall is thin. The pore size of the 15%S scaffold is about 50 μm, and the pore structure is uniform. The pore size of the 25%S scaffold was the smallest, with a thick pore wall and many obturator pores. With the increase in SF concentration, the pore size of porous scaffolds decreased gradually, and the pore wall thickened gradually.

The mechanical properties of scaffolds prepared with different concentrations of SF solution are shown in **Fig. S4b-d**. The compressive strength and elastic modulus of the 25%S scaffold are the highest, significantly higher than those of 5%S and 15%S scaffolds. It is mainly due to its low porosity and thick pore wall. The compressive strength and elastic modulus of the 15%S scaffold are significantly higher than those of the 5%S scaffold. Although the large pore structure of the 5%S scaffold may be conducive to cell infiltration and bone tissue growth, its small compressive strength leads to insufficient spatial maintenance ability, which is challenging to meet the needs of oral hard tissue repair under a complex compressive stress environment. Although the 25%S scaffold has the largest compressive strength and elastic modulus, its pore size is too small, the pore wall is thick, and some obturators exist, which is not

conducive to cell infiltration and bone tissue growth. Considering the scaffold's pore structure and mechanical properties, a 15% SF solution was selected to further construct the porous hybrid scaffold combined with chopped fibers and n-HA for subsequent research.

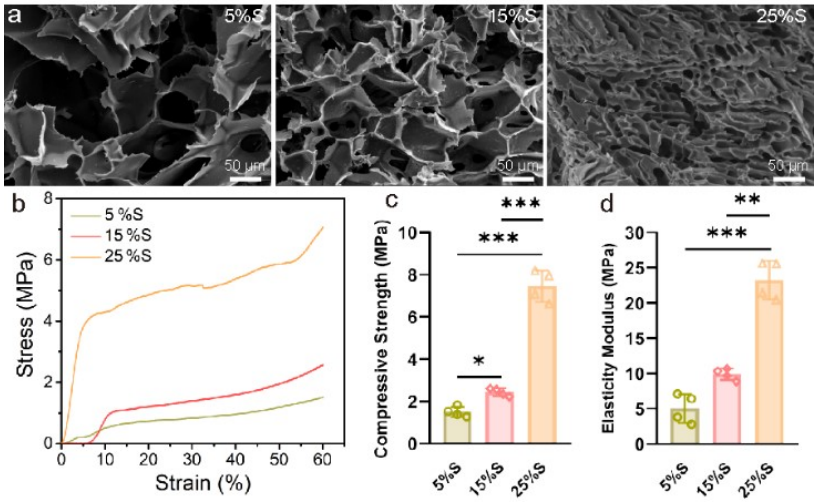

Fig. S4. The (a) SEM images and (b-d) compressive properties of pure silk fibroin porous scaffolds with different concentration solutions.

We detected the degradation rate. SH and SHCF scaffolds contain n-HA nanoparticles, which are released from the scaffolds during degradation, so the mass loss of SH and SHCF scaffolds is faster than that of S scaffold. However, the degradation rate of SHCF scaffold is slower than that of SH scaffold due to the bridging effect of chopped fibers.

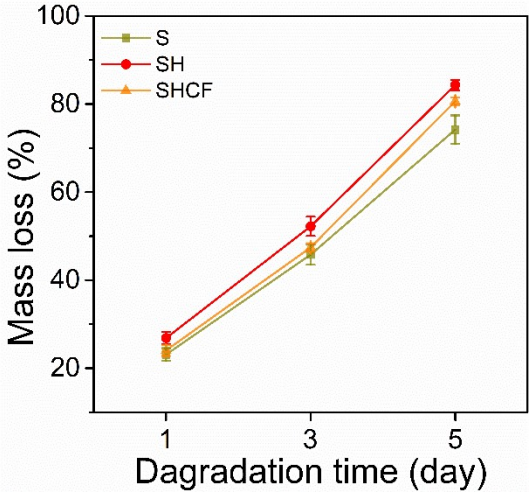

Fig. S5. Enzyme-induced degradation of S, SH and SHCF scaffolds.

The pearson correlation coefficients among S, SH, and SHCF groups were all greater than 0.9 (**Fig. S6a**). The gene expression analysis results of each group showed that there were 11601 same expression genes in the three groups. There were hundreds of differentially expressed genes among the three

groups (**Fig. S6b**). The cluster heatmap also visually showed the differential gene expression among the groups (**Fig. S6c**). A heat map of representative genes significantly upregulated in the SHCF group showed that the SHCF scaffold could upregulate the expression of genes related to the osteogenic process in BMSCs (**Fig. S6d**).

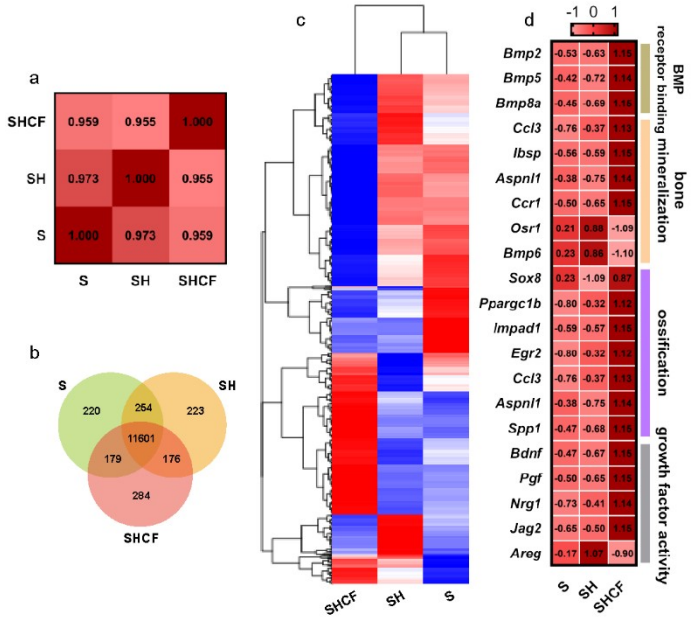

Fig. S6. Bulk-RNA-Seq results of BMSCs cultured on S, SH, and SHCF porous scaffolds for 14 d: (a) Pearson correlation coefficient, (b) Venn diagram, (c) Cluster heat map of differential genes, (d) Heatmap of the related gene expression of representative GO terms of SHCF group.

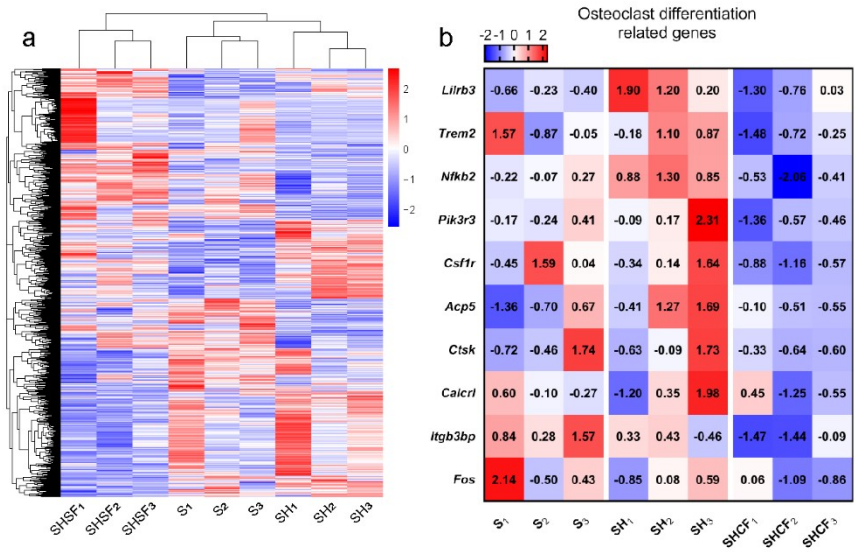

Fig. S7. Bulk-RNA-Seq of the S, SH, and SHCF scaffolds implanted in rat femur defects after two weeks: (a) cluster heat map of differential genes; (b) heatmap of the related gene expression of osteoclast differentiation.